Probing the Interplay between the Two Steps of Group I Intron Splicing: Competition of Exogenous Guanosine with ωG†

Patrick P. Zarrinkar‡ and Bruce A. Sullenger*,‡,§

Center for Genetic and Cellular Therapies, Department of Surgery, and Department of Genetics, Box 2601, Duke University Medical Center, Durham, North Carolina 27710

Received September 11, 1998; Revised Manuscript Received October 22, 1998

ABSTRACT: One largely unexplored question about group I intron splicing is how the cleavage and ligation steps of the reaction are coordinated. We describe a simple in vitro trans-splicing model system in which both steps take place, including the exchange of ligands in the guanosine-binding site that must occur between the two steps. Using this model system, we show that the switch is accomplished by modulating the relative affinity of the binding site for the two ligands. While the terminal guanosine of the intron (ωG) and exogenous guanosine compete for binding during the first step of splicing, no competition is apparent during the second step, when ωG is bound tightly. These results help explain how the ribozyme orchestrates progression through the splicing reaction. In addition to providing a new tool to ask basic questions about RNA catalysis, the trans-splicing model system will also facilitate the development of therapeutically useful group I ribozymes that can repair mutant mRNAs.

Ever since their discovery, group I introns have served as a model system to study RNA structure and function. Great progress has been made in elucidating the mechanism of action of these RNA enzymes (*1*, *2*), and an increasingly detailed view of their structure is emerging (*3*, *4*). Nevertheless, certain aspects of group I ribozyme catalysis remain poorly understood. The natural function of group I introns is to catalyze their own removal from precursor RNAs in a two step self-splicing reaction, in which cleavage at the 5′ splice site precedes exon ligation (Figure 1) (*5*). Splicing requires guanosine which binds to a specific site in the catalytic core of the ribozyme (*6*, *7*) and acts as the nucleophile during 5′ splice site cleavage (*8*). The same site is used to bind the terminal nucleotide of the intron, also a guanosine (frequently called ωG[1]), during exon ligation to help position and activate the 3′ splice site (*9*−*11*). Consequently, an exchange of ligands in the guanosine-binding site has to take place between the two steps (Figure 1). While there is direct evidence for several conformational changes between the two reaction steps in at least one group I intron (*12*) and for dynamic behavior of the guanosine-binding site (*10*, *13*−*19*), exactly how the ribozyme orchestrates this ligand switch remains largely unexplained.

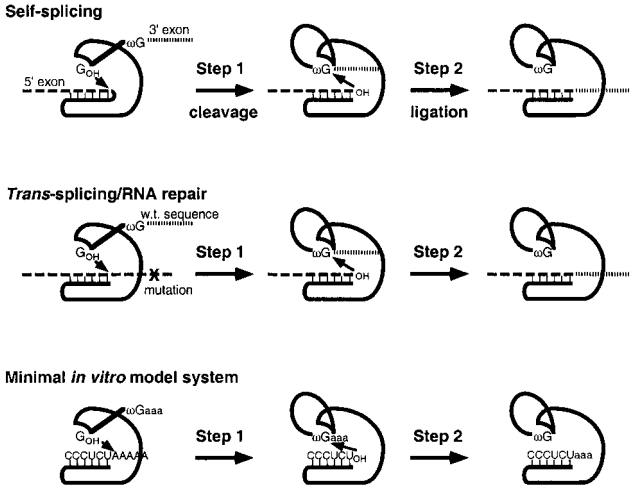

FIGURE 1: Group I intron splicing reactions. The intron is shown as a solid line and the exons as dashed lines. During the natural self-splicing reaction (top) 5′ splice site cleavage (step 1) precedes exon ligation (step 2). Exogenous guanosine serves as the nucleophile during the first step, and is displaced by ωG, which helps position the 3′ splice site for the second step. Trans-splicing (middle) is analogous to self-splicing except that the substrate RNA, which substitutes for the 5′ exon, is not covalently attached to the intron. RNA repair can be accomplished through trans-splicing if the initial cleavage takes place upstream of a mutation, and the mutated sequence is replaced with a wild-type version attached to the ribozyme as a 3′ exon. In a simple model for trans-splicing (bottom) a mutant sequence (AAAAA) in an oligonucleotide substrate is replaced by a shorter wild-type sequence (aaa).

In addition to serving as a model for basic investigations of RNA structure and catalysis, group I ribozymes may also be useful as RNA repair agents (*20*−*24*). Repair of mutant RNAs can be accomplished through a trans-splicing reaction analogous to self-splicing, but using an exogenous RNA as a substrate (*20*, *25*, *26*). The ribozyme first cleaves the

† Supported by NIH Grant GM 53525 (B.A.S.) and by a grant from the Jane Coffin Childs Memorial Fund for Medical Research. P.P.Z. is a Fellow of the Jane Coffin Childs Memorial Fund for Medical Research.

* To whom correspondence should be addressed. Phone: (919) 684 6375. Fax: (919)684 6492. E-mail: sulle001@mc.duke.edu.

‡ Center for Genetic and Cellular Therapies, Department of Surgery.

§ Department of Genetics.

[1] Abbreviations: ωG, terminal guanosine of the group I intron; pG, guanosine 5′-monophosphate; Tris, tris(hydroxymethyl)aminomethane; EDTA, ethylenediaminetetraacetic acid; MES, 2-(*N*-morpholino)-ethanesulfonic acid.

10.1021/bi982193x CCC: $15.00
Published on Web 12/01/1998

substrate upstream of the offending mutation, followed by ligation of a wild-type version of the removed sequence that is delivered by the ribozyme as its 3′ exon (Figure 1). While group I ribozyme-mediated RNA repair has been demonstrated both in vitro and in vivo (*20, 21, 23, 24*), significant improvements in ribozyme activity will most likely be required for this approach to become therapeutically viable (*27*). A necessary first step toward optimizing RNA repair in mammalian cells is to gain a greater understanding of the basic trans-splicing reaction in vitro.

We have therefore developed a minimal in vitro model system for trans-splicing that is derived from previously described approaches to study group I ribozyme catalysis (Figure 1) (*10, 17, 28, 29*). This system is unique in that both steps of splicing occur yet, unlike in self-splicing reactions, substrate and ribozyme can be manipulated independently. Furthermore, the complicating effects of long exons, which may form unfavorable intramolecular interactions that can interfere with self-splicing reactions (*30*−*33*), are avoided. The new system not only allows characterization of the RNA repair reaction, but also lends itself to a detailed examination of the interplay between the cleavage and ligation steps of splicing, including the exchange of ligands in the guanosine-binding site. We show that during the cleavage step exogenous guanosine competes with ωG for access to the guanosine-binding site. In contrast, during the ligation step, exogenous guanosine is unable to compete with ωG. The ribozyme therefore manipulates the relative affinities of the guanosine-binding site for free guanosine and ωG, thereby promoting progression of the splicing reaction in a sophisticated manner.

MATERIALS AND METHODS

Ribozymes. The L-21*Sca*I ribozyme was transcribed from plasmid pT7L-21 (*29*) linearized with *Sca*I. Transcription conditions were 40 mM Tris (pH 7.5), 25 mM $MgCl_2$, 2 mM spermidine, 10 mM dithiothreitol, 4 mM each nucleoside triphosphate, 500 units of T7 RNA polymerase, and 10 μg of linearized plasmid template/100 μL of volume. Transcription reactions were performed for 2.5 h at 37 °C. The L-21G414 ribozyme was transcribed from plasmid pT7L-21 linearized with *Nde*I, which produces a transcript with ∼200 nucleotides following G414 of the intron. Transcription was performed under the same conditions as for the L-21*Sca*I ribozyme, which are permissive for specific 3′ splice site hydrolysis. Hydrolysis results in a ribozyme ending with G414 as the 3′ terminal nucleotide that is significantly shorter than the unprocessed transcript, allowing easy separation on a polyacrylamide gel (*10*). The L-21A_3 ribozyme was transcribed using a template generated from plasmid pT7L-21 by PCR. The 5′ PCR primer (5′-ATT TCA CAC AGG AAA CAG CTA TG-3′) hybridizes upstream of the T7 promoter and was used directly as supplied by the manufacturer without further purification. The 3′ primer (5′-TTT CGA GTA CTC CAA AAC TAA TC-3′) is complementary to the last 20 nucleotides of the intron, ending with G414, followed by an overhang to encode the three adenosine residues that constitute the 3′ exon. The 3′ primer was purified on a 20% denaturing polyacrylamide gel before use to avoid size heterogeneity. PCR was performed with *Pfu* polymerase (Stratagene) which, unlike *Taq* polymerase, does not add nontemplated nucleotides and therefore further reduces the possibility of 3′ end heterogeneity in the final transcript. The use of *Pfu* polymerase, which has much higher fidelity than *Taq* polymerase, also decreases the likelihood of introducing unwanted mutations into the transcription template during PCR. PCR conditions were as recommended by the manufacturer [94 °C− 2 min (94 °C, 1 min; 60 °C, 1 min; 72 °C, 2 min) × 30 cycles, 72 °C, 10 min]. PCR products were phenol extracted and ethanol precipitated. Transcription conditions were as described above for the L-21*Sca*I and L-21G414 ribozymes, except that the $MgCl_2$ concentration was lowered to 5 mM to prevent 3′ splice site hydrolysis (*34*), and ∼0.5−1.5 μg of PCR product was used as the template in place of linearized plasmid. No significant 3′ splice site hydrolysis (<2% after 2.5 h) was detected when 3′-^{32}P-labeled L-21A_3 ribozyme was incubated under transcription conditions. Mutations were introduced by standard PCR methods, and transcription templates then were produced as described above for the wild-type ribozymes. Ribozymes were purified on 6% denaturing polyacrylamide gels, eluted overnight at 4 °C by soaking the gel slices in buffer (10 mM Tris, pH 7.5, 1 mM EDTA, and 0.3 M sodium acetate), and ethanol precipitated. Concentrations were determined by measuring the OD_{260}, assuming 1 OD_{260} = 40 μg/mL and using the molecular weight calculated from the ribozyme sequence.

Substrates. RNA oligonucleotide substrates were purchased from Dharmacon Research Inc. (Boulder, CO). They were deprotected according to the manufacturer's instructions and purified on 20% denaturing polyacrylamide gels. Thioeffects were measured with substrates having a mixture of R_p and S_p phosphorothioates at the cleavage site, taking into account the presence of the unreactive isomer when determining the observed rate constants (*14*). Concentrations were determined by measuring the OD_{260}, assuming 1 OD_{260} = 20 μg/mL (a conversion different than that used for the far larger ribozymes; see ref *35*). Substrates were 5′ end labeled using T4 polynucleotide kinase and a molar excess of γ-[^{32}P]-ATP (6000 Ci/mmol), purified as above and desalted on C_{18} cartridges (Waters). Concentrations were estimated by comparing the counts per unit volume of purified, labeled substrates to known standards of γ-[^{32}P]ATP using a Storm Imager (Molecular Dynamics) and assuming quantitative labeling.

Kinetics. All reactions were single turnover, using trace concentrations of 5′-^{32}P-labeled substrate (∼0.2 nM final concentration unless otherwise indicated) and ribozyme excess. Incubation of 3′-^{32}P-labeled L-21A_3 ribozyme under folding/reaction conditions revealed low or undetectable levels of 3′ splice site hydrolysis during the reaction times used in the experiments described (<10% at 37 °C, pH 7.5 after 20 min; < 5% at 50 °C, pH 5.5 after 4 h; < 1% at 37 °C, pH 5.5 after 20 min).

$(k_{cat}/K_m)^S$. Ribozyme in 20 μL of buffer (50 mM Tris, pH 7.5) was heated to 95 °C for 1 min, followed by addition of 20 μL of ice-cold buffer (50 mM Tris, pH 7.5, and 20 mM $MgCl_2$) containing enough magnesium to give a final concentration of 10 mM. The ribozyme was allowed to fold for three minutes at 37 °C before the reaction was initiated by adding substrate and guanosine 5′-monophosphate (final concentration 2 mM), preequilibrated for 4 min at 37 °C, in 40 μL of buffer (50 mM Tris, pH 7.5, and 10 mM $MgCl_2$). Reactions were performed at 37 °C. At least eight time points

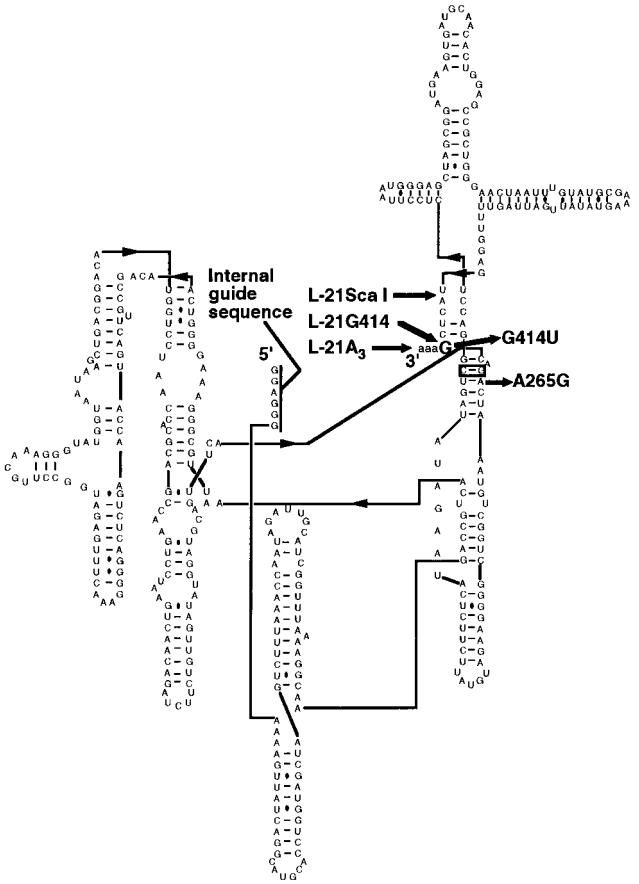

FIGURE 2: Secondary structure of the *Tetrahymena* ribozyme. The base pair proposed to interact with guanosine is boxed (*7*, *43*), and the internal guide sequence is indicated. The 3′ termini of the L-21*Sca*I, L-21G414, and L-21A_3 ribozymes and the mutations introduced at G414 and the guanosine-binding site are pointed out with arrows. The three adenosines of the 3′ exon in the L-21A_3 ribozyme are in lower case letters.

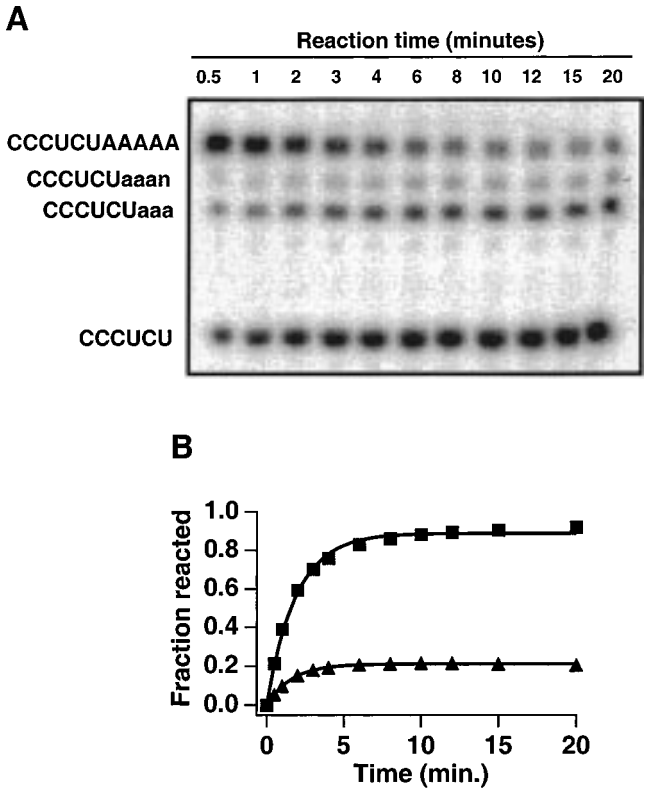

FIGURE 3: Trans-splicing catalyzed by the L-21A_3 ribozyme. The experiment was performed as described in the Materials and Methods for determination of $(k_{cat}/K_m)^S$ with a ribozyme concentration of 5 nM. (A) Image of a 20% denaturing polyacrylamide gel on which reaction products were separated. Substrate (CCCUCUAAAAA), intermediate (CCCUCU), and product (CCCUCUaaa and CCCUCUaaan) are clearly resolved. Lower case letters indicate nucleotides transferred from the 3′ exon of the L-21A_3 ribozyme (see Figure 1). A small fraction of the ribozyme contains a single nontemplated nucleotide (presumably added by T7 RNA polymerase) that follows the three template-encoded adenosines at the 3′ end, giving rise to the CCCUCUaaan product. Comparing the reaction shown here with reactions using the L-21*Sca*I ribozyme and the same preparation of labeled substrate indicates that all of the radioactivity migrating as CCCUCUAAAAA at the reaction endpoint (~10% of the input) is due to substrate that has not reacted, and not to the presence of product containing two nontemplated nucleotides transferred from the ribozyme. (B) Quantitation of the trans-splicing reaction shown in A. The first step (■) is analyzed by adding the fraction of intermediate (CCCUCU) and products (CCCUCUaaa and CCCUCUaaan added together; separate analysis shows that these two products behave identically, and can be treated as one), and plotting them as a function of reaction time. The second step (▲) is analyzed by plotting the fraction of products (CCCUCUaaa and CCCUCUaaan) as a function of time. The k_{obs} for the first and second step are 0.53 and 0.62 min^{-1}, respectively, and the endpoints are 0.89 for the first step and 0.21 for the second step.

were taken at regular intervals by removing 5 μL aliquots and adding them to 5 μL of stop solution (90 mM EDTA, 0.05% bromophenol blue, and 0.05% xylene cyanol in 88% formamide). Products were separated on 20% denaturing polyacrylamide gels and quantitated using a Storm Imager (Molecular Dynamics). The data were fit to single exponentials to obtain observed rate constants. To determine $(k_{cat}/K_m)^S$, at least four experiments were performed in the range where k_{obs} varies linearly with the ribozyme concentration. A plot of k_{obs} vs ribozyme concentration gives a straight line, and the slope is equal to $(k_{cat}/K_m)^S$. Doubling the pG concentration had no effect on k_{obs}, verifying that the pG concentration was saturating.

$(k_{cat}/K_m)^G$, k_c, $K_{1/2}^{pG}$. Experiments were as described for $(k_{cat}/K_m)^S$, except that MES (pH 5.5) was used instead of Tris as a buffer, ribozyme concentrations were saturating (100 nM; doubling the concentration had no effect on k_{obs}), and pG concentrations were varied appropriately. To determine $(k_{cat}/K_m)^G$ directly, at least four experiments were performed in the range where k_{obs} varies linearly with pG concentration. A plot of k_{obs} vs [pG] gives a straight line, and the slope is equal to $(k_{cat}/K_m)^G$. To determine k_c and $K_{1/2}^{pG}$, k_{obs} was measured over a broader range of pG concentrations (Figure 5), and the data fit to the equation $k_{obs} = [k_c[pG]/(K_{1/2}^{pG} + [pG])]$. Due to site-specific hydrolysis, there is still a very slow reaction in the absence of pG (*28*). The k_{obs} for hydrolysis was subtracted from the k_{obs} at each [pG], although this had no significant effect on the results.

Pulse-Chase Experiments. Reactions were performed as described above, with 50 mM MES (pH 5.5), except that the reaction and equilibration temperature was 50 °C. Concentrations during the pulse were 100 nM ribozyme, 4 mM pG, and 0.6 nM ^{32}P-labeled substrate. After 12 min, once the first step had gone to completion and the second step equilibrium had been established, part of the reaction was diluted 10-fold into a chase solution (50 mM MES, pH 5.5, and 10 mM $MgCl_2$) containing 2 μM unlabeled substrate. The reaction was then allowed to proceed at 50 °C. The value

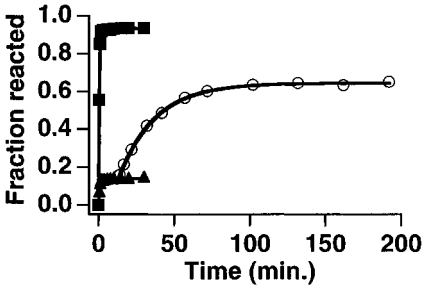

FIGURE 4: Pulse-chase experiment to probe the second step equilibrium. During the pulse phase (solid symbols) the equilibrium is established. (■) The fraction of substrate cleaved during the first step (CCCUCU); (▲) The product of second step ligation (CCCUCUaaa). Ligated product (CCCUCUaaa) accumulates during the chase phase (○).

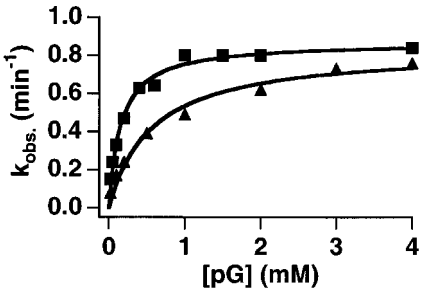

FIGURE 5: Guanosine binding to the L-21*Sca*I (■) and L-21A_3 (▲) ribozymes at 37 °C, 10 mM $MgCl_2$, pH 5.5. Experiments were performed at a series of pG concentrations and the data were fit as described in the Materials and Methods for determination of k_c and $K_{1/2}^{pG}$. Values for k_c and $K_{1/2}^{pG}$ are given in Table 1.

of k_{obs} for product accumulation during the chase depends on several microscopic rate constants (*10*), and conditions were chosen to maximize k_{obs} during the chase.

RESULTS

An in Vitro trans-Splicing System. For our investigations, we have used the *Tetrahymena* ribozyme, the most extensively studied group I intron (Figure 2) (*1, 2*). Two versions of this ribozyme have been previously described that can perform either the first or the second splicing step on short oligonucleotide substrates supplied in trans (Figures 1 and 2) (*29, 36*). The first version, called L-21*Sca*I, lacks the first 21 and the last five nucleotides of the full-length intron (Figure 2) (*29*). While it is capable of catalyzing the first step cleavage reaction, using guanosine (or guanosine 5′-monophosphate, pG) as a nucleophile, it is unable to catalyze exon ligation due to the lack of a 3′ exon and the 3′ terminal guanosine of the native intron (ωG, G414 in the *Tetrahymena* ribozyme) (*28, 29*). It has been argued that, if an oligonucleotide mimic of the 3′ splice site (UCGA) is provided as a substitute for ωG, the L-21*Sca*I ribozyme may also be used to model the second reaction step (*17, 37*). The second version of the *Tetrahymena* ribozyme, called L-21G414, retains the terminal five nucleotides of the intron (Figure 2) (*10*). It can catalyze the second splicing step in both the forward and reverse directions, using G414 as the nucleophile in the reverse reaction (see Figure 1), but still lacks the 3′ exon necessary to carry out both splicing steps (*10, 36*).

We reasoned that addition of a short 3′ exon to the L-21G414 ribozyme should allow it to catalyze both steps of a trans-splicing reaction. A ribozyme, which we call L-21A_3, was therefore generated that carries a 3′ exon consisting of three adenosine residues (Figure 2). This exon length was chosen to allow easy discrimination of the ligated trans-spliced product from both the substrate and the intermediate cleavage product, while avoiding any complications possible with longer exon sequences (*31*−*33*). Appropriate steps were taken to prevent excessive 3′ end heterogeneity and hydrolysis at the 3′ splice site during transcription, and control experiments showed that no significant 3′ splice site hydrolysis occurred during folding of the ribozyme or during the trans-splicing reactions (see Materials and Methods). The same short RNA oligonucleotide that has served as a substrate for the L-21*Sca*I (*28, 29*) and L-21G414 ribozymes (*10*) can be used by the L-21A_3 ribozyme. This oligonucleotide (CCCUCUAAAAA) consists of six nucleotides complementary to the internal guide sequence of the ribozyme (*38, 39*), followed by five adenosine residues. During the first step, the L-21A_3 ribozyme cleaves the substrate in a reaction equivalent to both the first step of splicing and the cleavage reaction catalyzed by the L-21*Sca*I ribozyme (*28, 29*). During the second step, the 3′ exon is ligated onto the upstream cleavage product in a reaction equivalent to the second step of splicing and the ligation reaction catalyzed by the L-21G414 ribozyme (Figure 1) (*10*). A representative experiment is shown in Figure 3. The substrate (CCCUCUAAAAA), intermediate (CCCUCU), and product (CCCUCUAAA) are all of different lengths and can be resolved on polyacrylamide gels (Figure 3A). From a single experiment, rate constants for each of the two reaction steps can be determined (Figure 3B). Both the intermediate and the final product represent substrate molecules that have undergone the first step, so k_{obs} for the first step (Figure 3B, squares) is obtained by plotting the sum of the fractions of intermediate and product versus time. The fraction of ligated product alone, plotted as a function of time, yields k_{obs} for the second step (Figure 3B, triangles). Since both steps take place, but can still be analyzed individually, the L-21A_3 ribozyme represents a useful tool to probe the interplay between the two steps of group I intron splicing.

The Second Step Equilibrium. Our first goal was to compare the reactions catalyzed by the L-21A_3 ribozyme with published results obtained using the L-21*Sca*I and L-21G414 variants described above. It was immediately apparent that while the first step in the L-21A_3 catalyzed reaction essentially goes to completion, not all of the intermediate proceeds through the second step (Figure 3). Experiments with the L-21G414 ribozyme have shown that the second step is readily and rapidly reversible and that an equilibrium is reached in which only a fraction of the substrate exists in the ligated state (*10*). To test whether a similar equilibrium is established with the L-21A_3 ribozyme, we performed a pulse-chase experiment as previously described (Figure 4) (*10*). A trace amount of ^{32}P-labeled substrate was added to a high concentration of ribozyme to permit rapid and complete binding, and the reaction was allowed to proceed until the first step had gone to completion and the putative second step equilibrium had been established (Figure 4, closed symbols). A large excess of unlabeled substrate was then added to prevent any intermediate or product that had dissociated from the ribozyme from rebinding. Since the ligated product is known to dissociate much faster than the

Table 1: Kinetic Constants for L-21*Sca*I and L-21A$_3$ Ribozymes

ribozyme	$(k_{cat}/K_m)^S$ [a] (M^{-1} min^{-1})	$K_{1/2}^{pG}$ [b] (mM)	k_c [b] (min^{-1})
L-21*Sca*I (wt)	$(1.06 \pm 0.23) \times 10^8$	0.16 ± 0.04	0.87 ± 0.05
L-21A$_3$ (wt)	$(0.86 \pm 0.22) \times 10^8$	0.56 ± 0.05	0.84 ± 0.03
L-21A$_3$ (G414U)	nd[c]	0.18 ± 0.01	0.80 ± 0.06

[a] Determined as described in the Materials and Methods at 37 °C, 10 mM $MgCl_2$, pH 7.5. The errors represent the range of values obtained when dividing k_{obs} by the ribozyme concentration for each concentration used. [b] From experiments shown in Figure 5 for the L-21*Sca*I(wt) and L-21A$_3$(wt) ribozymes, and from a similar experiment for the L-21A$_3$(G414U) ribozyme. The errors represent the range of values obtained in two independent sets of experiments. [c] Not determined.

intermediate, dissociated product is expected to accumulate during the chase phase of the experiment if there is indeed a rapid equilibrium (*10, 31*). Alternatively, if there is a second step defect, no increase of ligated product would be expected. Ligated product did accumulate during the chase, demonstrating that the incomplete conversion of intermediate to product is due to the reversibility of the second step and not to a fraction of the ribozyme being unable to perform the second step because of inactive conformations or loss of the 3′ exon (Figure 4, open symbols). Not all of the intermediate is eventually converted to product, however, presumably because some of the intermediate also dissociates from the ribozyme during the long chase. Parallel experiments with the L-21G414 ribozyme showed that under our conditions the position of the second step equilibrium, as well as the k_{obs} and extent of product accumulation during the chase were the same, within error, as for the L-21A$_3$ ribozyme (data not shown). The properties of the second step reaction catalyzed by the L-21A$_3$ ribozyme therefore are consistent with the intrinsic properties of the second step determined with the L-21G414 ribozyme (*10*).

Comparison of L-21ScaI and L-21A$_3$ Ribozymes. To evaluate the first splicing step catalyzed by the L-21A$_3$ ribozyme and compare it in more detail with the extremely well-characterized cleavage reaction catalyzed by the L-21*Sca*I ribozyme, we measured several kinetic constants that reflect individual steps along the reaction pathway. The second-order rate constant at low concentrations of ribozyme (E) and saturating concentrations of pG, $(k_{cat}/K_m)^S$, represents reaction of the ribozyme·pG complex with free substrate (E·pG + S). For the L-21*Sca*I ribozyme, $(k_{cat}/K_m)^S$ is limited by substrate binding and equivalent to k_{on} for the substrate (*28*). The values of $(k_{cat}/K_m)^S$ for the L-21A$_3$ and L-21*Sca*I ribozymes are the same, within error, and agree well with previously published results (Table 1) (*28, 40*). A pulse-chase experiment, as described (*28*), confirmed that under these conditions substrate binding is also rate limiting for the L-21A$_3$ ribozyme (data not shown).

Lowering the pH from 7.5 to 5.5 slows down the chemical cleavage step, and at saturating concentrations of ribozyme and pG, k_{obs} equals k_c, the rate constant for the chemical step (*13, 40*). Furthermore, the $K_{1/2}$ for pG ($K_{1/2}^{pG}$) at low pH and saturating concentrations of ribozyme is equal to its dissociation constant (K_d^{pG}) from the ribozyme·substrate complex (*13, 14*) and is therefore sensitive to effects on guanosine binding. The value of k_c for the L-21*Sca*I and L-21A$_3$ ribozymes was the same, within error, and consistent with previously published results (Table 1) (*13, 40*), suggesting that the rate of chemistry is not affected by the presence of a 3′ exon. However, while the $K_{1/2}^{pG}$ for the L-21*Sca*I ribozyme was also similar to published results (*13*), an almost 4-fold increase was observed for the L-21A$_3$ ribozyme (Figure 5, Table 1). Together, these results demonstrate that while there appear to be no fundamental differences in the cleavage reaction catalyzed by the L-21A$_3$ and L-21*Sca*I ribozymes, the presence of the terminal five nucleotides of the intron and a 3′ exon does seem to have an effect on binding of exogenous guanosine.

Competition between Exogenous Guanosine and ωG during the First Step. At least three explanations for the apparently weaker binding of exogenous guanosine to the L-21A$_3$ ribozyme are possible. One, a change in the rate-limiting step has occurred, and $K_{1/2}^{pG}$ does not equal K_d^{pG} for the L-21A$_3$ ribozyme under these conditions. Two, guanosine binding to the longer L-21A$_3$ ribozyme may be intrinsically weaker, compared to the truncated L-21*Sca*I version. Three, the terminal guanosine of the intron (ωG), which is absent in the L-21*Sca*I ribozyme (Figure 2) but has to bind to the guanosine-binding site during the second step of splicing in the L-21A$_3$ ribozyme, competes with free guanosine during the first step.

To test whether the chemical step remains rate limiting for the L-21A$_3$ ribozyme, we measured the effect of replacing the phosphate at the cleavage site in the oligonucleotide substrate with a phosphorothioate. This substitution results in a thio-effect, a small but distinct decrease in the observed rate constant, if chemistry is rate limiting (*14, 41*). We observed a thio-effect of similar magnitude for the L-21A$_3$ and L-21*Sca*I ribozymes, measured in side-by-side reactions, at pG concentrations both below and above the $K_{1/2}^{pG}$ [2.4 ± 0.7 and 2.8 ± 0.4, respectively, at low pG (0.1 mM), 1.5 ± 0.01 and 1.6 ± 0.1, respectively, at high pG (similar values were observed at 2 mM and 4 mM pG); the errors encompass the range of values obtained in two independent experiments]. Combined with the absence of a lag in product formation and the confirmation that ribozyme concentrations were saturating (see Materials and Methods), this suggests that chemistry remains rate limiting and is consistent with $K_{1/2}^{pG} = K_d^{pG}$ for both the L-21A$_3$ and the L-21*Sca*I ribozymes (*13*). The difference in $K_{1/2}^{pG}$ values between the L-21*Sca*I and L-21A$_3$ ribozymes therefore is most likely due to a difference in guanosine binding and not a change in the rate-limiting step.

To distinguish between the remaining two possibilities, we mutated ωG to U (G414U) (Figure 2). A uracil in the terminal position of the intron is unable to occupy the guanosine-binding site and prevents the ribozyme from carrying out the second step of the reaction (*42*). If guanosine binding to L-21A$_3$ is intrinsically weaker than binding to L-21*Sca*I because of the additional nucleotides, then the G414U mutation should have little effect on $K_{1/2}^{pG}$. If, however, weaker apparent binding is due to competition between ωG and exogenous guanosine, the mutation should restore $K_{1/2}^{pG}$ to that found for the L-21*Sca*I ribozyme. The $K_{1/2}^{pG}$ for the L-21A$_3$(G414U) ribozyme is decreased compared to L-21A$_3$(wt) and within error of that observed for L-21*Sca*I (Table 1). No significant change in k_c is observed, showing that the mutation does not affect the chemical rate of the first step. These results are consistent with the hypothesis that there is competition between exogenous

Table 2: Effect of Mutating ωG or the Guanosine-Binding Site on Binding of Exogenous Guanosine

	$(k_{cat}/K_m)^G$ (M^{-1} min^{-1})		
ribozyme	L-21*Sca*I	L-21A_3	L-21*Sca*I/L-21A_3[c]
wt[a]	5.4×10^3	1.5×10^3	3.6 ± 1.0
G414U[a]	5.4×10^3	4.4×10^3	1.2 ± 0.3
A265G[b]	41 ± 8	27 ± 4	1.5 ± 0.4

[a] Calculated from $K_{1/2}^{pG}$ and k_c in Table 1. [b] Determined as described in Materials and Methods at 37 °C, 10 mM $MgCl_2$, pH 5.5. The errors represent the range of values obtained in two independent sets of experiments. [c] Ratios of $(k_{cat}/K_m)^G$ for the L-21*Sca*I and L-21A_3 versions of the ribozymes. Errors were determined by standard propagation of the errors in experimentally determined values for k_c, $K_{1/2}^{pG}$ (wt and G414U), or $(k_{cat}/K_m)^G$ (A265G).

guanosine and G414 for access to the guanosine-binding site during the cleavage step of the splicing reaction.

As a further test of the competition hypothesis, we also determined the effect of mutating the guanosine-binding site. Guanosine binding requires the interaction of guanosine with a base pair in the ribozyme core (Figure 2) (*7, 43*) as well as a second contact with an adjacent nucleotide (A265) (*43, 44*). To weaken, but not abolish, guanosine binding, we mutated A265 to G (Figure 2) (*43*). If there is competition between exogenous guanosine and ωG, then the ratio of $K_{1/2}^{pG}$ for the L-21A_3 and L-21*Sca*I versions of the A265G mutant ribozyme should be lower than it is for the two versions of the wild-type ribozyme. This would be expected because, while weaker binding of exogenous guanosine can be overcome by increasing the free guanosine concentration, the effective concentration of ωG is fixed and the ribozyme cannot compensate for the decreased affinity of the guanosine-binding site for ωG.

Due to the significantly weaker binding of pG to the A265G mutant, it was not possible to accurately determine the k_c and $K_{1/2}^{pG}$ individually, as shown for the wild-type ribozymes in Figure 5. Instead, we determined the second-order rate constant at saturating ribozyme concentrations and subsaturating pG concentrations, $(k_{cat}/K_m)^G$, which represents reaction of the ribozyme·substrate complex with free pG (E·S + pG) (Table 2). $(k_{cat}/K_m)^G$ corresponds to the slope of the linear portion (at low concentrations of pG) of a plot such as that shown in Figure 5, and therefore is sensitive to changes in both k_{cat} (= k_c) and $K_{1/2}^{pG}$.

Compared to the L-21*Sca*I(wt) ribozyme, $(k_{cat}/K_m)^G$ for the L-21*Sca*I(A265G) ribozyme is reduced more than 100-fold (Table 2). Although complete saturation could not be achieved, k_{obs} for the A265G mutant at high pG concentrations begins to approach k_c measured for the wild-type ribozyme (less than a 2-fold difference at 15 mM pG; data not shown). The lower $(k_{cat}/K_m)^G$ therefore likely reflects largely an increase in $K_{1/2}^{pG}$ and weaker pG binding, as expected, rather than an effect on the chemical step. Similarly, since k_c is almost the same for the wild-type and the G414U ribozymes (see Table 1), differences in $(k_{cat}/K_m)^G$ directly reflect differences in $K_{1/2}^{pG}$ (Table 2). While the ratio of $(k_{cat}/K_m)^G$ for the L-21*Sca*I and L-21A_3 versions of the ribozyme is 3.6 for the wild-type (Table 2), reflecting the difference in $K_{1/2}^{pG}$'s (Table 1), it is close to one for both the G414U and A265G mutants (Table 2).

Mutating either the terminal nucleotide of the intron or the guanosine-binding site therefore significantly decreases the apparent difference in guanosine-binding affinity between the L-21*Sca*I and L-21A_3 versions of the ribozyme. These observations support the proposal that an interaction between the terminal nucleotide and the guanosine-binding site is responsible for that difference in the wild-type ribozymes. Together, these results strongly suggest that during the first step of splicing exogenous guanosine competes with ωG for access to the guanosine-binding site and ωG essentially acts as an intramolecular competitive inhibitor. While it is most likely that the competition is direct, it cannot presently be completely ruled out that ωG alters the affinity of the guanosine-binding site for exogenous guanosine and therefore competes indirectly.

No Competition between Exogenous Guanosine and ωG during the Second Step. Since there is competition for access to the guanosine-binding site during the first step, we wanted to test whether this is also the case during the second step. At low pH, where chemistry is rate limiting, k_{obs} for the first step is dependent on the fraction of ribozyme that has exogenous pG bound (see Figure 5) (*13*), since pG has to be present to act as a nucleophile. Similarly, the second step can only proceed when ωG is bound in the guanosine-binding site, and the k_{obs} is expected to depend on the fraction of ribozyme having ωG bound (*10*). If competition exists between ωG and exogenous pG during the second step of splicing, increasing the concentration of free pG would be expected to displace ωG from the guanosine-binding site. This would result in a decrease in k_{obs} for the second step, whereas k_{obs} for the first step should continue to increase until saturating concentrations of pG are reached and k_{obs} equals k_c. We therefore compared k_{obs} for the first (Figure 6A, closed symbols) and second steps (Figure 6A, open symbols) at increasing concentrations of pG. No decrease in k_{obs} for the second step was observed even at high pG concentrations. Instead, k_{obs} for the second step increases with increasing pG concentrations and is almost identical to k_{obs} for the first step at all guanosine concentrations tested. This result is consistent with a lack of competition between ωG and exogenous pG during the second step. However, since k_{obs} for the first and second steps are the same (see legend of Figure 6), the first step appears to be overall rate limiting, and k_{obs} for the second step does not really reflect the intrinsic rate constant of the second step. The second step may be very rapid, consistent with earlier results (*10*), and therefore even a substantial decrease in its intrinsic rate constant at high pG concentrations may not be detected because the first step remains overall rate limiting.

To determine the effect of increasing pG concentrations on the rate constant of the second step more directly, we took advantage of the flexibility of the trans-splicing system and initiated the reaction by addition of the six nucleotide intermediate (CCCUCU) instead of the standard 11 nucleotide substrate (CCCUCUAAAAA) (Figure 1). The L-21A_3 ribozyme can perform the second step directly on this intermediate, bypassing the first step. In the absence of exogenous pG (Figure 6B, closed symbols), reaction with the intermediate was fast and proceeded to the same equilibrium endpoint as the second step in the context of the two step reaction initiated with the standard substrate. The presence of 4 mM pG had no effect (Figure 6B, open symbols), and even 10 mM pG, a concentration at which the guanosine-binding site is saturated with exogenous pG

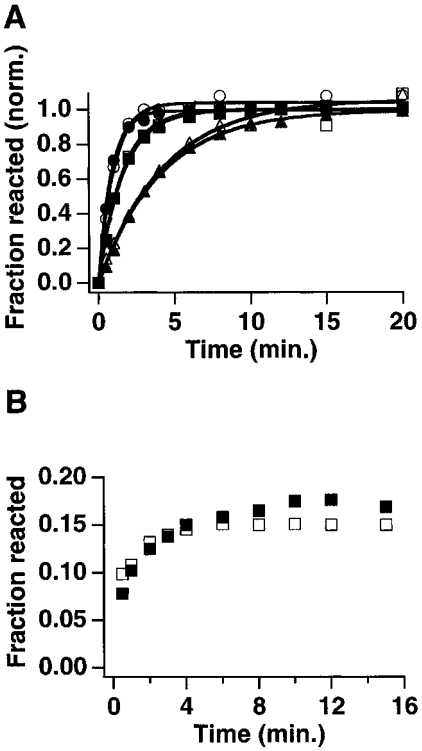

FIGURE 6: Probing the second step of trans-splicing. (A) Time courses of trans-splicing at 37 °C, 10 mM $MgCl_2$, pH 5.5 with 100 nM L-21A_3 ribozyme in the presence of 0.2 mM (triangles), 2 mM (squares), and 10 mM (circles) pG. To allow a direct comparison, the data for the first and second step at each pG concentration were normalized by correcting for the different endpoints. The k_{obs} for the first and second steps, respectively, were 0.25 min^{-1} (▲) and 0.25 min^{-1} (△) at 0.2 mM pG, 0.63 min^{-1} (■) and 0.62 min^{-1} (□) at 2 mM pG, 1.2 min^{-1} (●) and 0.99 min^{-1} (○) at 10 mM pG. (B) Time course of reaction of the L-21A_3 ribozyme with CCCUCU in the presence of 0 mM (■) and 4 mM (□) pG. Conditions were the same as in panel A, except that reactions were performed at room temperature to slow the reaction. The first step is bypassed and only the second step occurs (CCCUCU → CCCUCUaaa), reaching an equilibrium similar to that in the two-step reaction (see Figure 3).

during the first step (Figure 5), did not reduce the apparent rate of the second step reaction (data not shown). Although we cannot completely rule out that a conformational change remains rate limiting even during the second-step-only reaction at pH 5.5, together these observations suggest that exogenous pG is unable to compete with ωG for occupancy of the guanosine-binding site during the second step.

DISCUSSION

A trans-Splicing System to Study the Interplay between the Two Reaction Steps. One aspect of group I intron splicing that is only now beginning to be addressed is the interplay between the two reaction steps (*10, 12, 17, 31*). We have developed a minimal in vitro trans-splicing system that lends itself to the exploration of this issue (Figure 1). While the previously described L-21*Sca*I and L-21G414 ribozymes (*10, 29, 36*) were engineered to perform either the first or the second step of the splicing reaction, the L-21A_3 ribozyme described here can catalyze both steps if supplied with a standard substrate (Figure 3) or the second step only if supplied with a shorter substrate corresponding to the product of the first step (Figure 6B). The trans-splicing reaction is analogous to the two step self-splicing reaction, except that the 3′ end of the substrate is not covalently attached to the intron prior to the cleavage step (Figure 1). With the L-21A_3 ribozyme, there is no need for long exon sequences, which may complicate analysis of self-splicing reactions (*30, 32, 33*). In addition, the concentrations of substrate and ribozyme can still be varied independently and the substrate can be chemically synthesized to introduce defined functional group mutations, allowing in-depth kinetic analysis of the interplay between the two steps of the splicing reaction. The L-21A_3, L-21*Sca*I, and L-21G414 variants of the *Tetrahymena* ribozyme complement each other, with each best suited to probe distinct details of group I ribozyme catalysis.

Exchange of Ligands in the Guanosine-Binding Site between the Two Steps. We have used the L-21A_3 ribozyme to explore the exchange of ligands in the guanosine-binding site that must take place between the two steps of group I intron splicing. Exogenous guanosine is bound during the first step and serves as the nucleophile during cleavage, while during the second step, binding of ωG helps position the 3′ splice site for attack (*45*). We show that during the first step of splicing exogenous pG has to compete with ωG for access to the binding site, resulting in an apparent weakening of pG binding (Figure 5). Mutating either ωG or the guanosine-binding site to destabilize the competing interaction restores binding to the level observed for the L-21*Sca*I ribozyme, which lacks ωG (Tables 1 and 2). In contrast to the competition observed during the first step, even high concentrations of exogenous pG have no apparent effect on the second step, indicating that ωG is tightly bound and does not have to compete with pG (Figure 6).

The results presented here are consistent with earlier observations showing that, in the context of the L-21*Sca*I ribozyme, complex reciprocal effects exist between binding of 5′ exon analogues and guanosine (*13, 15, 16*). The affinity of the ribozyme·substrate complex (corresponding to the state preceding the first step) for exogenous guanosine has been demonstrated to be higher than that of the ribozyme· intermediate complex (the intermediate being the product of the first step, and this complex therefore corresponding to the state preceding the second step), prompting the proposal that if binding of ωG is not similarly affected, the change in affinity for exogenous guanosine should promote progression of the splicing reaction (*13*). We now provide direct evidence in support of this proposal. Our results are also consistent with observations using the L-21G414 ribozyme, which models the second step of the reaction, where exogenous guanosine was virtually unable to compete with ωG (*10*), as well as with the suggestion that tight binding of ωG after completion of the second step may prevent exon reopening (*11*). While it is known that binding of ωG with a 3′ exon attached is significantly weaker than without an attached exon (*10, 46*), it appears that even with an attached exon ωG can bind tight enough to deny exogenous guanosine access to the guanosine-binding site during the second step.

The emerging picture suggests that the *Tetrahymena* group I ribozyme employs a mechanism for exchanging ligands in the guanosine-binding site that involves fine tuning the relative affinities for the two ligands as the reaction proceeds. While the affinity for exogenous guanosine appears to decrease between the first and second steps (*13*), the affinity for ωG may not change at all or may even increase. Presumably, this modulation is accomplished through subtle

conformational changes, for which evidence exists in another group I intron (*12*), and which may be responsible for differences that have been observed in the active site during the first and second steps (*47*). What exactly these conformational changes are and how they modulate the relative affinities remains an open question.

A Model System for RNA Repair. The trans-splicing system was also developed to provide a simplified version of group I ribozyme-mediated RNA repair (*20*−*22*), a potential new therapeutic approach to amend genetic information at the RNA level (Figure 1) (*23*, *24*). The L-21A_3 ribozyme not only allows a detailed characterization of the repair reaction, a likely prerequisite for interpreting results of in vivo experiments, but also makes it possible to gauge the effects of changes introduced into the ribozyme that are designed to improve in vivo activity. Such changes may include mutations that alter the intrinsic activity of the ribozyme, for example to increase its specificity (P.P.Z. and B.A.S., submitted for publication), which is low both in vitro (*29*, *48*, *49*) and in vivo (*21*) (P.P.Z. and B.A.S., unpublished observation), as well as insertion of sequences to promote efficient expression in mammalian cells, or colocalization with intended substrates in specific subcellular compartments (*50*). In summary, the minimal in vitro trans-splicing system described here provides a tool to study aspects of group I ribozyme catalysis not easily accessible with other systems, as well as a means to rationally improve the ability of the *Tetrahymena* ribozyme to repair defective RNAs.

ACKNOWLEDGMENT

We thank D. Herschlag, C. Rusconi, M. Long, and L. Milich for helpful discussions and critical reading of the manuscript, A. M. Pyle for helpful discussions, and T. Cech for providing plasmid pT7L-21.

REFERENCES

1. Cech, T. R., and Herschlag, D. (1996) in *Catalytic RNA* (Eckstein, F., and Lilley, D. M. J., Eds.) pp 1−17, Springer-Verlag, Berlin, Heidelberg.
2. Narlikar, G. J., and Herschlag, D. (1997) *Annu. Rev. Biochem. 66*, 19−59.
3. Cate, J. H., Gooding, A. R., Podell, E., Zhou, K., Golden, B. L., Kundrot, C. E., Cech, T. R., and Doudna, J. A. (1996) *Science 273*, 1678−1685.
4. Lehnert, V., Jaeger, L., Michel, F., and Westhof, E. (1996) *Chem. Biol. 3*, 993−1009.
5. Cech, T. R. (1993) in *The RNA World* (Gesteland, R. F., and Atkins, J. F., Eds.) pp 239−269, Cold Spring Harbor Laboratory Press, Plainview, NY.
6. Bass, B. L., and Cech, T. R. (1984) *Nature 308*, 820−826.
7. Michel, F., Hanna, M., Green, R., Bartel, D. P., and Szostak, J. W. (1989) *Nature 342*, 391−395.
8. Cech, T. R., Zaug, A. J., and Grabowski, P. J. (1981) *Cell 27*, 487−496.
9. Been, M. D., and Perrotta, A. T. (1991) *Science 252*, 434−437.
10. Mei, R., and Herschlag, D. (1996) *Biochemistry 35*, 5796−5809.
11. Suh, E., and Waring, R. B. (1993) *J. Mol. Biol. 232*, 375−385.
12. Golden, B. L., and Cech, T. R. (1996) *Biochemistry 35*, 3754−3763.
13. McConnell, T. S., Cech, T. R., and Herschlag, D. (1993) *Proc. Natl. Acad. Sci. U.S.A. 90*, 8362−8366.
14. McConnell, T. S., and Cech, T. R. (1995) *Biochemistry 34*, 4056−4067.
15. Bevilacqua, P. C., Johnson, K. A., and Turner, D. H. (1993) *Proc. Natl. Acad. Sci. U.S.A. 90*, 8357−8361.
16. Bevilacqua, P. C., Li, Y., and Turner, D. H. (1994) *Biochemistry 33*, 11340−11348.
17. Bevilacqua, P. C., Sugimoto, N., and Turner, D. H. (1996) *Biochemistry 35*, 648−658.
18. Profenno, L. A., Kierzek, R., Testa, S. M., and Turner, D. H. (1997) *Biochemistry 36*, 12477−12485.
19. Emerick, V. L., and Woodson, S. A. (1994) *Proc. Natl. Acad. Sci. U.S.A. 91*, 9675−9679.
20. Sullenger, B. A., and Cech, T. R. (1994) *Nature 371*, 619−622.
21. Jones, J. T., Lee, S.-W., and Sullenger, B. A. (1996) *Nat. Med. 2*, 643−648.
22. Jones, J. T., and Sullenger, B. A. (1997) *Nat. Biotechnol. 15*, 902−905.
23. Lan, N., Howrey, R. P., Lee, S.-W., Smith, C. A., and Sullenger, B. A. (1998) *Science 280*, 1593−1596.
24. Phylactou, L. A., Darrah, C., and Wood, M. J. A. (1998) *Nat. Gen. 18*, 378−381.
25. Inoue, T., Sullivan, F. X., and Cech, T. R. (1985) *Cell 43*, 431−437.
26. Emerick, V. L., and Woodson, S. A. (1993) *Biochemistry 32*, 14062−14067.
27. Sullenger, B. A. (1995) *Chem. Biol. 2*, 249−253.
28. Herschlag, D., and Cech, T. R. (1990) *Biochemistry 29*, 10159−10171.
29. Zaug, A. J., Grosshans, C. A., and Cech, T. R. (1988) *Biochemistry 27*, 8924−8931.
30. Woodson, S. A., and Cech, T. R. (1991) *Biochemistry 30*, 2042−2050.
31. Emerick, V. L., Pan, J., and Woodson, S. A. (1996) *Biochemistry 35*, 13469−13477.
32. Nolte, A., Chanfreau, G., and Jacquier, A. (1998) *RNA 4*, 694−708.
33. Semrad, K., and Schroeder, R. (1998) *Genes Dev. 12*, 1327−1337.
34. Zaug, A. J., McEvoy, M. M., and Cech, T. R. (1993) *Biochemistry 32*, 7946−7953.
35. Sambrook, J., Fritsch, E. F., and Maniatis, T. (1989) *Molecular cloning: A laboratory manual*, Cold Spring Harbor Laboratory Press, Plainview, NY.
36. Robertson, D. L., and Joyce, G. F. (1990) *Nature 344*, 467−468.
37. Weinstein, L. B., Jones, B. C. N. M., Cosstick, R., and Cech, T. R. (1997) *Nature 388*, 805−808.
38. Been, M. D., and Cech, T. R. (1986) *Cell 47*, 207−216.
39. Waring, R. B., Towner, P., Minter, S. J., and Davies, R. W. (1986) *Nature 321*, 133−139.
40. Strobel, S. A., and Cech, T. R. (1993) *Biochemistry 32*, 13593−13604.
41. Herschlag, D., Piccirilli, J. A., and Cech, T. R. (1991) *Biochemistry 30*, 4844−4854.
42. Price, J. V., and Cech, T. R. (1988) *Genes Dev. 2*, 1439−1447.
43. Yarus, M., Illangesekare, M., and Christian, E. (1991) *J. Mol. Biol. 222*, 995−1012.
44. Ortoleva-Donnelly, L., Szewczak, A. A., Gutell, R. R., and Strobel, S. A. (1998) *RNA 4*, 498−519.
45. Cech, T. R. (1990) *Annu. Rev. Biochem. 59*, 543−568.
46. Moran, S., Kierzek, R., and Turner, D. H. (1993) *Biochemistry 32*, 5247−5256.
47. Strobel, S. A., and Shetty, K. (1997) *Proc. Natl. Acad. Sci. U.S.A. 94*, 2903−2908.
48. Herschlag, D., and Cech, T. R. (1990) *Biochemistry 29*, 10172−10180.
49. Young, B., Herschlag, D., and Cech, T. R. (1991) *Cell 67*, 1007−1019.
50. Sullenger, B. A., and Cech, T. R. (1993) *Science 262*, 1566−1569.

BI982193X